PERGAMON

International Journal of Solids and Structures 39 (2002) 4027–4037

INTERNATIONAL JOURNAL OF SOLIDS and STRUCTURES

www.elsevier.com/locate/ijsolstr

Stress wave propagation in orthotropic laminated thick-walled spherical shells

X. Wang [a,*], G. Lu [b], S.R. Guillow [b]

[a] *Department of Engineering Mechanics, The School of Civil Engineering and Mechanics, Shanghai Jiaotong University, Shanghai 200240, P.R. China*

[b] *School of Engineering and Science, Swinburne University of Technology, Hawthorn, Vic. 3122, Australia*

Received 6 September 2001; received in revised form 18 January 2002

Abstract

This paper presents an elastodynamic solution for stress wave propagation in an orthotropic laminated spherical shells with arbitrary thickness. The elastodynamic equation for each separate orthotropic spherical shell is solved by means of finite Hankel transforms and Laplace transforms. Then by using the interface continuity conditions between layers and the boundary conditions at the internal and external surfaces of the laminated shells we determine the unknown constants involved. Thus an exact solution for stress wave propagation in orthotropic laminated spherical shells subjected to arbitrary radial dynamic load is obtained.

Keywords: Composite laminated structures; Elastodynamic stress; Stress wave propagation

1. Introduction

The investigation of stress wave propagation in hollow spherical or cylindrical structures subjected to exterior or interior time-dependent pressure is a typical elastodynamic problem. Solution of this problem has various useful engineering applications, such as non-destructive evaluations of material properties, flaw detection in structures and determination of resonance frequencies. In the past, a number of analytical solutions for stress wave propagation in a structure consisting of a single isotropic material have been obtained by Huth (1955), Baker (1961), Baker et al. (1966), Torvic (1967), Achenbach and Fang (1970), Mchinney (1971) and Pao (1983). However the investigation of stress wave propagation in a laminated structure subjected to shock loading is a more complex problem which so far the subject has not been investigated as extensively as it deserves.

Yu (1960), Chu (1961) and Bieriek and Freudenthal (1962) studied vibrations in laminated shells using a Timoshenko-type theory. This limited application to thin laminated shell-type structures and this method was only used to calculate vibrations in laminated structures. Cho et al. (1998) presented an elastodynamic

* Corresponding author.
E-mail address: xwang@mail.sjtu.edu.cn (X. Wang).

0020-7683/02/$ - see front matter
PII: S0020-7683(02)00264-0

solution for the thermal shock stresses in an orthotropic thick-wall cylindrical shell. Wang et al. (2000) presented both theoretical and finite element solutions for an orthotropic thick-wall cylindrical shell under impact load. Piskunov et al. (1994) developed improved transverse shear and normal deformation higher-order theory for the solution of dynamic problem involving multilayered plates and shells with an arbitrary number and sequence of transverse isotropic layers. Tabiei et al. (1999) used the finite element approach to investigate the behaviour of cylindrical laminated shells when acted upon by a sudden dynamic load. Shakeri et al. (1999) solved for dynamic response of an axisymmetric laminated composite cylindrical shell of finite length. He used higher-order shear deformation theory and trigonometric function expansion in the axial direction.

In this paper the equations for stress wave propagation in an orthotropic laminated thick-walled spherical shell are developed and solved by using a finite integral transform method. Firstly, the governing equations for each orthotropic layer of the laminated spherical shells are derived and then solved by means of finite Hankel transforms and Laplace transforms. The basic solution for the governing equation of each separate orthotropic layer is composed of a quasi-static solution with unknown constants and a dynamic solution meeting the homogeneous boundary conditions. From the interface continuity requirements between laminated layers and the internal and external boundary conditions of the laminated spherical thick-wall shell, we can easily determine the unknown constants involved in this solution. Therefore an exact solution for stress wave propagation in an orthotropic laminated spherical thick-wall shell is obtained. This solution is illustrated with numerical examples to demonstrate that the methodology is simple to apply and theoretically valid.

2. Elastodynamic solution for orthotropic laminated thick-walled spherical shell

Consider an orthotropic laminated thick-walled spherical shell (fiber reinforced spherical vessel) acted on by dynamic internal pressure, $\psi(t)$, which is uniformly distributed over the internal surface. This investigation is most conveniently carried out by using spherical coordinate system (r, θ, φ) with the origin at the centre of the spherical shell. The material of each separate layer in the laminated thick-walled spherical shell is assumed to possess transverse isotropy (fiber reinforced spherical vessel) about any radius vector drawn from the common centre of the spherical shell to a given point. It is obvious that for the elastic properties indicated, the distribution of stress and strain depends only on the radial variable r, and all points are displaced only in the radial direction during deformation. $U^j(r)$ denotes the single (radial) component of displacement of each separating layer. The geometry of the shell structure is shown in Fig. 1, where a_1 and b_n are respectively the internal radii and the external radii of the complete spherical shell. a_j and b_j $(j = 1, 2, \ldots, n)$ as shown in Fig. 1, represent respectively the internal radii and the external radii of the j layer of the laminated shell. In Fig. 1, we have

$$a_j = b_{j-1} \quad (j = 1, 2, \ldots, n) \tag{1}$$

Assuming that the laminated spherical thick-wall shell is subjected to an arbitrary dynamic internal pressure, $\psi(t)$, the orthotropic elastodynamic equation of the jth layer of the spherical thick-walled shell may be obtained as per Lekniskii (1981)

$$\frac{\partial^2 U^j(r,t)}{\partial r^2} + \frac{2}{r}\frac{\partial U^j(r,t)}{\partial r} - 2\frac{A^j_{22} + A^j_{23} - A^j_{12}}{A^j_{11}}\frac{U^j(r,t)}{r^2} = \frac{1}{V_j^2}\frac{\partial^2 U^j(r,t)}{\partial t^2} \quad (a_j \leqslant r \leqslant b_j;\ t \geqslant 0) \tag{2a}$$

where $U^j(r,t)$ expresses the single (radial) component of displacement in the jth layer, $V_j = \sqrt{A^j_{11}/\rho_j}$ is the spherical wave speed in the jth layer and ρ_j is the density in the jth layer. Elastic constants, A^j_{kl}, in the above formula are related to E_j and v_j in the j layer as follows:

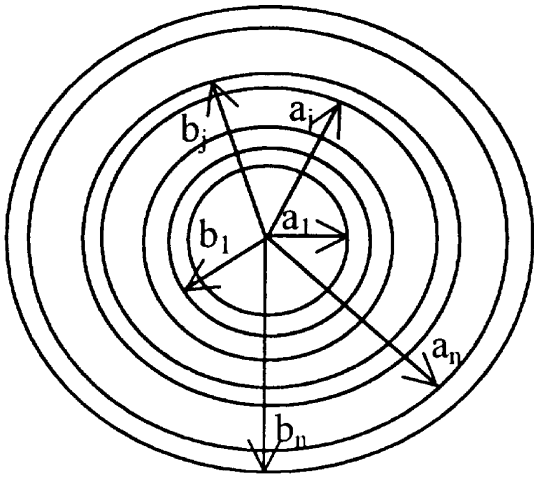

Fig. 1. Geometrical structure of laminated thick-walled spherical shells.

$$A_{11}^j = \frac{E_r^j(1-v_\theta^j)}{m}, \quad A_{12}^j = \frac{E_\theta^j v_r^j}{m}, \quad A_{22}^j = \frac{E_\theta^j}{(1+v_\theta^j)m}\left(1-(v_r^j)^2\frac{E_\theta^j}{E_r^j}\right),$$
$$A_{23}^j = \frac{E_\theta^j}{(1+v_\theta^j)m}\left[v_\theta^j + (v_r^j)^2\frac{E_\theta^j}{E_r^j}\right], \quad m = 1 - v_\theta^j - 2(v_r^j)^2\frac{E_\theta^j}{E_r^j} \tag{2b}$$

where E_r^j and E_θ^j are Young's modulus for tension along and perpendicular to the radius vector, r, respectively. v_r^j is Poisson's ratio for transverse contraction in a direction perpendicular to r when tension is applied in the r direction and v_θ^j is Poisson's ratio for contraction in a plane normal to radius vector, r, for tension in the same plane.

The initial condition for Eqs. (2a) and (2b) may be written as

$$U^j(r,0) = U_0^j(r), \quad \frac{\partial U^j(r,o)}{\partial t} = V_0^j(r) \tag{3}$$

Boundary and continuity conditions between interfaces of the laminated spherical shell may be expressed as internal boundary condition:

$$\sigma_r^1(a_1,t) = \psi(t) \tag{4a}$$

external boundary condition:

$$\sigma_r^n(b_n,t) = 0 \tag{4b}$$

displacement continuity condition between layers:

$$U^j(b_j,t) = U^{j+1}(a_{j+1},t), \quad (j = 1,2,\ldots,n-1) \tag{4c}$$

Stress continuity condition between layers:

$$\sigma_r^j(b_j,t) = \sigma_r^{j+1}(a_{j+1},t), \quad (j = 1,2,\ldots,n-1) \tag{4d}$$

Utilizing geometrical relation and generalized Hooke's law, dynamic stresses in the jth layer are given by

$$\sigma_r^j(r,t) = A_{11}^j\frac{\partial U^j}{\partial r} + 2A_{12}^j\frac{U^j(r,t)}{r} \tag{5a}$$

$$\sigma_\theta^j(r,t) = A_{12}^j \frac{\partial U^j}{\partial r} + (A_{22}^j + A_{23}^j)\frac{U^j(r,t)}{r} \tag{5b}$$

Assume that the general solution of Eqs. (2a) and (2b) is of the form

$$U^j(r,t) = U_s^j(r,t) + U_d^j(r,t) \tag{6}$$

where $U_s^j(r,t)$ is the quasi-static part and $U_d^j(r,t)$ is the dynamic part of the solution. Assume that the static term $U_s^j(r,t)$ satisfy the following equations

$$\frac{\partial^2 U_s^j(r,t)}{\partial r^2} + \frac{2}{r}\frac{\partial U_s^j(r,t)}{\partial r} - 2\frac{A_{22}^j + A_{23}^j - A_{13}^j}{A_{11}^j}\frac{U_s^j(r,t)}{r^2} = 0 \tag{7a}$$

$$U_s^j(r,0) = 0, \quad \frac{\partial U_s^j(r,o)}{\partial t} = 0 \tag{7b}$$

Applying general integral to Eq. (7a) yields

$$U_s^j(r,t) = \varphi_1^j(r)\psi(t) \tag{8}$$

where

$$\varphi_1^j(r) = C_1^j r^{k-0.5} + C_2^j r^{-k-0.5} \tag{9a}$$

$$k = \sqrt{0.25 + 2(A_{22}^j + A_{23}^j - A_{12}^j)/A_{11}^j} \tag{9b}$$

In Eqs. (8), (9a) and (9b) the independent constants of integration are C_1^j and C_2^j. These constants can be determined by considering boundary conditions at the internal and external surfaces and continuity conditions at laminated interfaces.

Substituting Eq. (6) into (5a) and (5b) and utilizing Eqs. (7a) and (7b) provides an inhomogeneous dynamic equation with homogeneous boundary conditions from which we can determine the dynamic solution term $U_d^j(r,t)$ for the jth layer.

$$\frac{\partial^2 U_d^j(r,t)}{\partial r^2} + \frac{2}{r}\frac{\partial U_d^j(r,t)}{\partial r} - 2\frac{A_{22}^j + A_{23}^j - A_{13}^j}{A_{11}^j}\frac{U_d^j(r,t)}{r^2} = \frac{1}{V_j^2}\left[\frac{\partial^2 U_d^j(r,t)}{\partial t^2} - \frac{\partial^2 U_s^j(r,t)}{\partial t^2}\right] \tag{10a}$$

$$A_{11}^j \frac{\partial U_d^j(a,t)}{\partial r} + 2A_{12}^j \frac{U_d^j(a,t)}{a} = 0, \qquad A_{11}^j \frac{\partial U_d^j(b,t)}{\partial r} + 2A_{12}^j \frac{U_d^j(b,t)}{b} = 0 \tag{10b, c}$$

$$U_d^j(r,0) = 0, \quad \dot{U}_d^j(r,0) = 0 \tag{10d, e}$$

Suppose that

$$U_d^j(r,t) = r^{-1/2} f^j(r,t) \tag{11}$$

Substituting Eq. (11) into (10a), (10b,c) and (10d,e) gives

$$\frac{\partial^2 f^j(r,t)}{\partial r^2} + \frac{1}{r}\frac{\partial f^j(r,t)}{\partial r} - k^2\frac{f^j(r,t)}{r^2} = \frac{1}{V_j^2}\left[\frac{\partial^2 f^j(r,t)}{\partial t^2} - \frac{\partial^2 U_{s1}^j(r,t)}{\partial t^2}\right] \tag{12a}$$

$$\left[\frac{\partial f^j(r,t)}{\partial r} + \frac{4A_{12}^j - A_{11}^j}{2A_{12}^j} f^j(r,t)\right]_{r=a_j,b_j} = 0 \tag{12b, c}$$

$$f^j(r,0)=0, \quad \dot{f}^j(r,0)=0 \tag{12d, e}$$

where

$$U^j_{s1}(r,t)=r^{-1/2}U^j_s(r,t) \tag{13}$$

and $U^j_s(r,t)$ is the known quasi-static solution shown in Eq. (8). Let $U^j_{s1}(r,t)=0$ in Eq. (12a) then this homogeneous equation with homogeneous boundary conditions (12b,c) may be solved by assuming

$$f^j_0(r,t)=g(r)\exp(\mathrm{i}\omega t) \tag{14}$$

From Eqs. (12a), (12b,c) and (12d,e) and (14) we have the following eigenequation

$$Y_aJ_b-Y_bJ_a=0 \tag{15a}$$

where

$$Y_a=\xi_iY'_k(\xi_ia)+h_{a_j}Y_k(\xi_ia), \qquad J_a=\xi_iJ'_k(\xi_ia)+h_{a_j}J_k(\xi_ia)$$

$$Y_b=\xi_iY'_k(\xi_ib)+h_{b_j}Y_k(\xi_ib), \qquad J_b=\xi_iJ'_k(\xi_ib)+h_{b_j}J_k(\xi_ib)$$

and

$$h_{a_j}=\frac{4A^j_{12}-A^j_{11}}{2a_jA^j_{11}}, \qquad h_{b_j}=\frac{4A^j_{12}-A^j_{11}}{2b_jA^j_{11}} \tag{15b–g}$$

where $J_k(\xi_ir)$ and $Y_k(\xi_ir)$ are kth-order Bessel functions of the first and second kinds respectively. In the above formula ξ_i $(i=1,2,\ldots,n)$ express a series of positive roots of the natural eigenequation (15a).

Define a finite Hankel transform $f(r,t)$ such that

$$\bar{f}(\xi_i,t)=H[f(r,t)]=\int_a^b rf(r,t)G_k(\xi_it)\,\mathrm{d}r \tag{16}$$

Then the inverse Hankel transform is given by

$$f(r,t)=\sum_i F(\xi_i)\bar{f}(\xi_i,t)G_k(\xi_ir) \tag{17}$$

where

$$F(\xi_i)=1\Big/\int_{a_j}^{b_j} r[G_k(\xi_ir)]^2\,\mathrm{d}r \tag{18a}$$

$$G_k(\xi_ir)=J_k(\xi_ir)Y_a-Y_k(\xi_ir)J_a \tag{18b}$$

Applying the finite Hankel transform (16) to Eq. (12a) we have

$$\frac{2}{\pi}\frac{J^j_a}{J^j_b}[f^j(b_j)+h_{b_j}f^j(b_j)]-\frac{2}{\pi}[f^j(a_j)+h_{a_j}f^j(a_j)]-\xi^j_i\bar{f}^j(\xi_i,t)=\frac{1}{V^2_j}\left[\frac{\partial^2\bar{f}^j}{\partial t^2}+\frac{\partial^2\overline{U}^j_{s1}}{\partial t^2}\right] \tag{19a}$$

where

$$\overline{U}^j_{s1}=H[U^j_{s1}(r,t)] \tag{19b}$$

The first two terms on the left hand side of Eq. (19a) should be zero in view of the homogeneous boundary condition Eq. (12b,c). Thus Eq. (19a) simplifies to

$$-\xi_i^j \bar{f}^j(\xi_i,t) = \frac{1}{V_j^2}\left[\frac{\partial^2 \bar{f}^j(\xi_i,t)}{\partial t^2} + \frac{\partial^2 \overline{U}_{s1}^j(\xi_i,t)}{\partial t^2}\right] \tag{20}$$

Applying Laplace transforms to Eq. (20) we have

$$\bar{f}^{j*}(\xi_i,p) = -\overline{U}_{s1}^j(\xi_i,p) + \frac{(\xi_i V_j)^2}{(\xi_i V_j)^2 + p^2}\overline{U}_{s1}^{j*}(\xi_i,p) \tag{21}$$

where p is the Laplace transform parameter. The inverse Laplace transform to Eq. (21) gives

$$\bar{f}^j(\xi_i^j,t) = \bar{\varphi}(\xi_i^j) I^j(\xi_i^j,t) \tag{22a}$$

where

$$I^j(\xi_i^j,t) = -\psi(t) + \xi_i^j V_j \int_0^t \psi(\tau)\sin[\xi_i^j V_j(t-\tau)]\,\mathrm{d}\tau \tag{22b}$$

$$\bar{\varphi}(\xi_i^j) = H[r^{1/2}\varphi_1(r)] = C_1^j R_1^j + C_2^j R_2^j \tag{22c}$$

$$R_1^j = H[r^k], \quad R_2^j = H[r^{-k}] \tag{22d}$$

Substituting Eqs. (22a)–(22d) into Eq. (17) and utilizing Eq. (11), the solution to (10a), (10b,c) and (10d,e) can be expressed as

$$U_d^j(r,t) = C_1^j \sum_i \left[FRI_1^j G_{kR}(\xi_i^j r)\right] + C_2^j \sum_i \left[FRI_2^j G_{kR}(\xi_i^j r)\right] \tag{23a}$$

where

$$FRI_1^j = R_1^j I^j(\xi_i^j,t)F(\xi_i^j), \qquad FRI_2^j = R_2^j I^j(\xi_i^j,t)F(\xi_i^j) \tag{23b}$$

$$G_{kR}(\xi_i^j) = r^{-1/2}G_k(\xi_i^j) \tag{23c}$$

From Eqs. (6), (8), (23a), (23b) and (23c), the solution to the orthotropic elastodynamic Eqs. (2a) and (2b) for the jth layer may be expressed as

$$U^j(r,t) = C_1^j\left\{r^{k-0.5}\psi(t) + \sum_i \left[FRI_1^j G_{kR}^j(\xi_i^j)\right]\right\} + C_2^j\left\{r^{-k-0.5}\psi(t) + \sum_i \left[FRI_2^j G_{kR}^j(\xi_i^j r)\right]\right\} \tag{24}$$

Substituting Eq. (24) into Eqs. (5a) and (5b) gives exact expressions for general stress solutions as follows

$$\begin{aligned}
\sigma_r^j(r,t) = {} & \{[A_{11}^j(k-0.5)+A_{12}^j]r^{k-1.5}C_1^j + [A_{11}^j(-k-0.5)+A_{12}^j]r^{-k-1.5}C_2^j\}\psi(t) \\
& + C_1^j \sum_i \left\{FRI_1^j\left[A_{11}^j\frac{\mathrm{d}G_{kR}^j(\xi_i^j r)}{\mathrm{d}r} + A_{12}^j\frac{G_{kR}^j(\xi_i^j r)}{r}\right]\right\} + C_2^j\sum_i\left\{FRI_2^j\left[A_{11}^j\frac{\mathrm{d}G_{kR}^j(\xi_i^j r)}{\mathrm{d}r} + A_{12}^j\frac{G_{kR}^j(\xi_i^j r)}{r}\right]\right\} \\
\sigma_\theta^j(r,t) = {} & \left\{\left[A_{12}^j(k-0.5)+A_{22}^j+A_{23}^j\right]r^{k-1.5}C_1^j + \left[A_{11}^j(-k-0.5)+A_{22}^j+A_{23}^j\right]r^{-k-1.5}C_2^j\right\}\psi(t) \\
& + C_1^j\sum_i\left\{FRI_1^j\left[A_{12}^j\frac{\mathrm{d}G_{kR}^j(\xi_i^j)}{\mathrm{d}r} + (A_{22}^j+A_{23}^j)\frac{G_{kR}^j(\xi_i^j r)}{r}\right]\right\} \\
& + C_2^j\sum_i\left\{FRI_2^j\left[A_{12}^j\frac{\mathrm{d}G_{kR}^j(\xi_i^j)}{\mathrm{d}r} + (A_{22}^j+A_{23}^j)\frac{G_{kR}^j(\xi_i^j r)}{r}\right]\right\}
\end{aligned} \tag{25a,b}$$

In the above solutions there are $2n$ undetermined constants, C_1^j, C_2^j $(j = 1,2,\ldots,n)$. Substituting the general stress solutions (24) and (25a,b) into the boundary conditions and interface continuity conditions (4a)–(4d) we have:at the internal boundary, $r = a_1$:

$$[A_{11}^1(k_1-0.5)+A_{12}^1]a_1^{k_1-1.5}C_1^1+[A_{11}^1(-k_1-0.5)+A_{12}^1]a_1^{-k_1-1.5}C_2^1=1 \tag{26a}$$

at the external boundary, $r=b_n$:

$$[A_{11}^n(k_n-0.5)+A_{12}^n]b_n^{k_n-1.5}C_1^n+[A_{11}^n(-k_n-0.5)+A_{12}^n]b_n^{-k_n-1.5}C_2^n=0 \tag{26b}$$

stress must be continuous at the interface $r=a_{j+1}=b_j$:

$$\begin{aligned}&[A_{11}^j(k_j-0.5)+A_{12}^j]b_j^{k_j-1.5}C_1^j+[A_{11}^j(-k_j-0.5)+A_{12}^j]b_j^{-k_j-1.5}C_2^j\\&\quad=[A_{11}^{j+1}(k_{j+1}-0.5)+A_{12}^{j+1}]a_{j+1}^{k_{j+1}-1.5}C_1^{j+1}+[A_{11}^{j+1}(-k_{j+1}-0.5)+A_{12}^{j+1}]a_{j+1}^{-k_{j+1}-1.5}C_2^{j+1}\end{aligned} \tag{26c}$$

displacement must be continuous at the interface $r=a_{j+1}=b_j$:

$$\begin{aligned}&C_1^j\left\{b_j^{k_j-0.5}\psi(t)+\sum_i\left[FRI_1^jG_{kR}^j(\xi_i^jb_j)\right]\right\}+C_2^j\left\{b_j^{-k_j-0.5}\psi(t)+\sum_i\left[FRI_2^jG_{kR}^j(\xi_i^jb_j)\right]\right\}\\&=C_1^j\left\{a_{j+1}^{-k_{j+1}-0.5}\psi(t)+\sum_i\left[FRI_1^{j+1}G_{kR}^{j+1}(\xi_i^{j+1}a_{j+1})\right]\right\}+C_2^j\left\{a_{j+1}^{-k_{j+1}-0.5}\psi(t)+\sum_i\left[FRI_2^{j+1}G_{kR}^{j+1}(\xi_i^{j+1}a_{j+1})\right]\right\}\end{aligned} \tag{26d}$$

where $j=1,2,\ldots,n-1$. There are just $2n$ linear equations in Eqs. (26a)–(26d), which are used to determine the $2n$ constants C_1^j and C_2^j $(j=1,2,\ldots,n)$. Thus an exact expression for the stress response for an orthotropic laminated spherical shell with n layers is obtained.

3. Numerical examples and discussions

As an example, calculations were carried out for two cases of orthotropic laminated spherical shells of fiber reinforced layers and a metal liner as follows: $_{\text{inter}}$[Aluminium/T300 carbon fiber] and $_{\text{inter}}$[Aluminium/Glass fiber/T300 carbon fiber]. It was assumed that the orientation of fiber reinforcement layers was such that there was transverse isotropy along any radius vector drawn from the common centre of the spherical shell. The material properties and the mass density for each layer of the laminated spherical shells are as follows: (1) T300 carbon fiber layer: $E_{\text{T}\theta}=180$ GPa, $E_{\text{T}\theta}/E_{\text{T}r}=1.875$, $v_{\text{T}r}=v_{\text{T}\theta}=0.21$, $\rho_{\text{T}}=0.018$ N/cm^3. (2) Glass fiber layer: $E_{\text{G}\theta}=80$ GPa, $E_{\text{G}\theta}/E_{\text{G}r}=3$, $v_{\text{G}r}=v_{\text{G}\theta}=0.25$, $\rho_{\text{G}}=0.024$ N/cm^3. (3) Aluminium layer: $E=70$ GPa, $v=0.33$, $\rho=0.027$ N/cm^3.

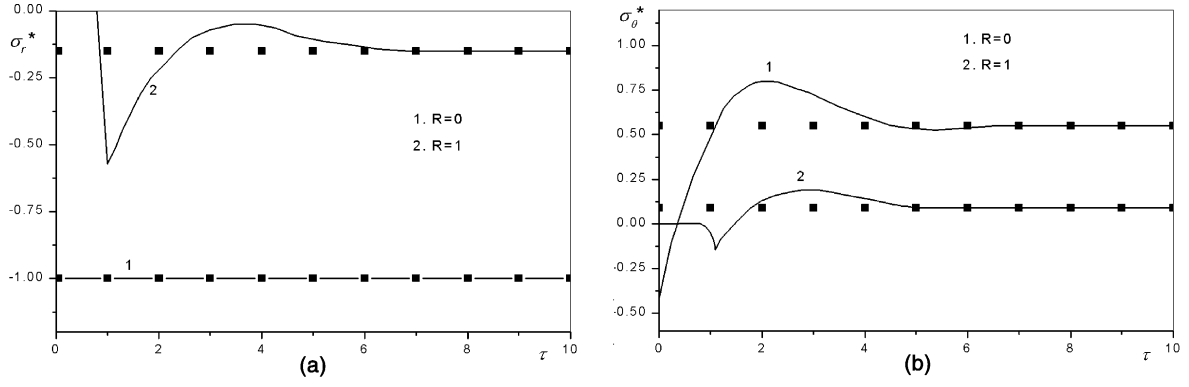

Fig. 2. Responses and distributions of the dynamic stress in the laminated thick-walled spherical shells [Aluminium/T300 fiber], without the interference of reflected wave. (■) indicates the corresponding quasi-static solution. $R=(r-a_1)/a_1$, $\tau=tV_1/a_1$, $\sigma_i^*=\sigma_i/p$.

Assume that the internal boundary only of the fiber reinforced laminated shell is subjected to a sudden uniform pressure load $\psi(t)$. In this case we have

$$\psi(t) = \begin{cases} 0 & t < 0^- \\ -p & t > 0^+ \end{cases} \tag{27}$$

In all results presented the following expressions have been used: normalised stresses $\sigma_i^* = \sigma_i/p$, normalised radii $R = (r - a_1)/a_1$ and $R_1 = (r - a_1)/(b_n - a_1)$, time period $T = t\sum_j^n V_j/(b_j - a_j)$ $(j = 1, 2, \ldots, n)$, $(n = 2$ or 3), and sample (■) indicates the corresponding quasi-static solution.

In order to verify the correctness of the solution presented in this paper consider the following. As a first example consider the dynamic response of a laminated spherical shell having two layers $_{\text{inter}}$[Aluminium/T300 fiber] where the geometry is such that $(b_1 - a_1)/a_1 = 10$ and $(b_2 - a_1)/a_1 = 20$. The calculated time was taken as $0 \leqslant \tau = tV_1/a_1 \leqslant 10$ to avoid the influence of reflected waves at the laminated interface or the internal and external boundaries. Fig. 2 shows the response histories of radial and tangential stresses at $r = a_1$ and $2a_1$. As shown in Fig. 2(a) curve 1, the radial dynamic stress at the internal boundary $(r = a_1)$ of fiber reinforced laminated spherical shell is $\sigma_r^* = -1$. This shows that the boundary condition (4a) has been rigorously satisfied.

From Fig. 2(a) and (b) we can see that before the stress wavefront arrives at a point in the fiber reinforced laminated shell, the dynamic stress at this point equals zero. When the stress wavefront arrives at this point, there is a strong discontinuity in stress and the stress reaches its maximum value at this point. As the stress wavefront moves past this point toward the external boundary, the stress wave oscillations at the

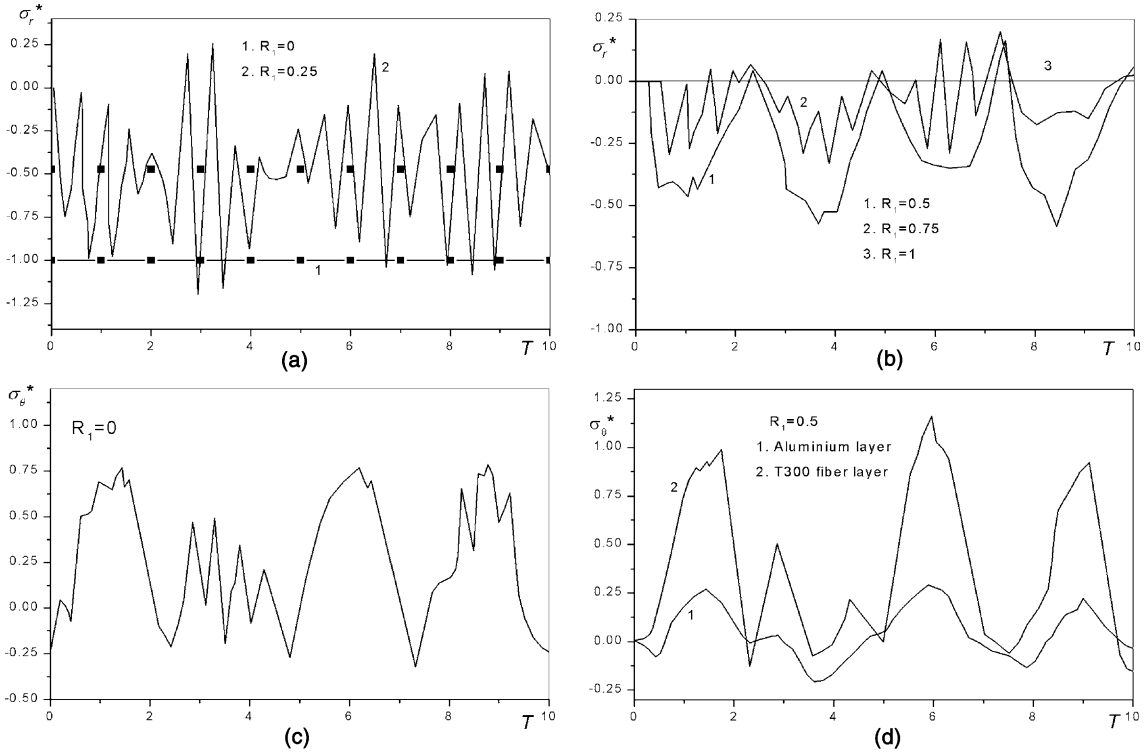

Fig. 3. Responses and distributions of the dynamic stress in the laminated thick-walled spherical shells [Aluminium/T300 fiber]. (■) indicates the corresponding quasi-static solution. $R_1 = (r - a_1)/(b_2 - a_1)$, $T = t\sum_j^2 V_j/(b_j - a_j)$, $\sigma_i^* = \sigma_i/p$.

point gradually decrease and finally the stress equals the corresponding quasi-static value at the same point. From the above analysis we can conclude that the proposed elastodynamic solution for orthotropic laminated thick-walled spherical shell is valid and has the wave characteristics. At the point of the strong discontinuity, the sign for tangential stress at the wavefront is opposite to the sign of static tangential stress, which is similar for the result of an isotropic hollow sphere under sudden load found by Miklowitz (1966).

As a second example consider a two layer laminated spherical shell as before $_{\text{inter}}$[Aluminium/T300] but with geometry $(b_1 - a_1)/a_1 = 0.5$ and $(b_2 - a_1)/a_1 = 1$. Fig. 3 shows the response histories and distributions of dynamic stress for such a shell. From Fig. 3(a) curve 1 and Fig. 3(b) curve 3, we can see that the

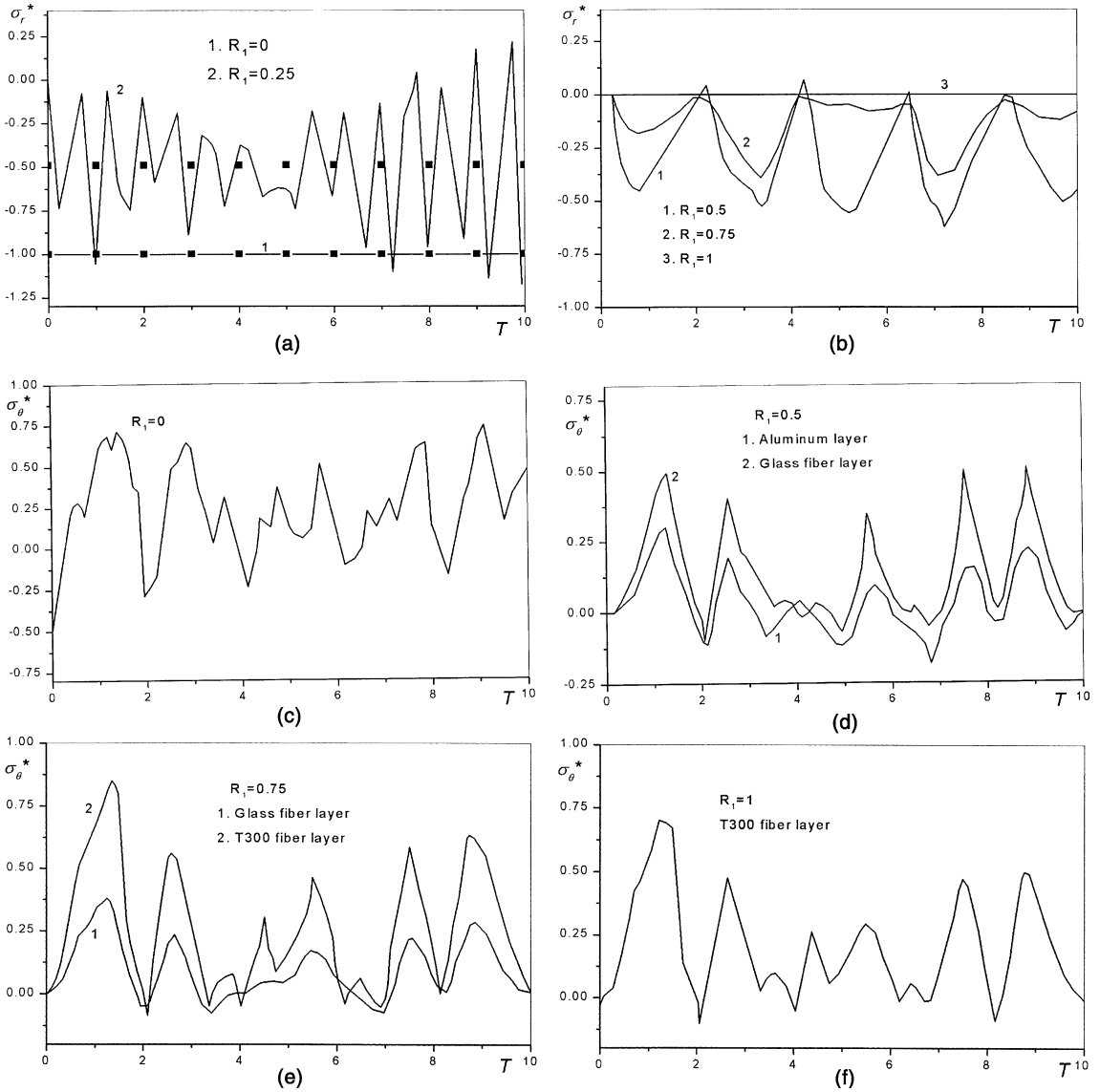

Fig. 4. Responses and distributions of the dynamic stress in the sandwich thick-walled spherical shell [Aluminium/Glass fiber/T300 fiber]. (■) indicates the corresponding quasi-static solution. $R_1 = (r - a_1)/(b_3 - a_1)$, $T = t\sum_j^3 V_j/(b_j - a_j)$, $\sigma_i^* = \sigma_i/p$.

radial dynamic stresses at the internal and external boundaries rigorously satisfy the given boundary conditions, at Eqs. (4a) and (4b). Because of the influence of stress wave reflected at the internal and external boundaries and the laminated interface, the dynamic stresses at every point in the spherical shell appear at a strong oscillation as time T and the abrupt changes in the curves. It can be seen from Fig. 3(a) and (b) that the maximum radial stress is at the middle of aluminium layer ($R = 0.25$) in the laminated shell. Radial stress at the lamination interface is continuous, which satisfies the given continuity condition Eq. (4d). For most response histories, radial dynamic stress at the interface ($R_1 = 0.5$) appears as a compressive stress wave but at some response histories, the radial dynamic stress at the interface appear as a tensile stress wave which might easily induce delamination failure of the laminated spherical shell.

Fig. 3(c) shows the response history for tangential stress at the internal boundary of the laminated shell. Fig. 3(d) shows the response history for tangential stress at the interface of the laminated shell. Tangential stress at the laminated interface appears as a discontinuity. Tangential stiffness of the T300-carbon fiber layer is much larger than the tangential stiffness of the aluminium layer, hence tangential stress at the laminated interface of the T300-carbon fiber layer is much larger than the corresponding tangential stress in aluminium. Comparing Fig. 3(c) and (d), we can see that the maximum tangential dynamic stress appears at the laminated interface in T300 fiber layer. This is different from the response history for a spherical shell constructed from a single material, where the maximum dynamic tangential stress occurs at the inner boundary.

As a third example consider a laminated spherical shell with three layers: $_{\text{inter}}$[Aluminium/Glass/T300] and geometry $(b_1 - a_1)/a_1 = 0.5$, $(b_2 - a_1)/a_1 = 0.75$ and $(b_3 - a_1)/a_1 = 1$. The corresponding response histories are shown in Fig. 4. The maximum radial dynamic stress still appears at the middle point $R_1 = 0.25$ of the first layer (Aluminium liner) and radial dynamic stress gradually decreases as the radius r increases. The radial dynamic stress at two laminated interfaces is continuous compressive stress wave. This will not easily induce delamination failure at the interface of this laminated spherical shell. Because the stiffness of the T300-carbon fiber layer is much larger than that of other two layers, the maximum tangential dynamic stress appears at the second interface between the T300 and glass fiber layers. Comparing Figs. 3 and 4, it can be seen that the response histories and distribution of dynamic stress in an orthotropic laminated spherical shell are influenced by lamination material and pattern of lamination.

It can be concluded that the major accomplishment of this study has been to provide a better solution method for stress wave propagation in fiber reinforced laminated spherical shells. This dynamic analysis method may be applied to a wide range of laminated structural shells. According to engineering requirements, this method may be used to rationally select lamination material and laying pattern in the design of laminated spherical shell structures subjected to shock loading. On the other hand, given the dynamic response signal of stress waves in a laminated spherical shell we can deduce the laying pattern and material properties of lamination.

References

Achenbach, J.D., Fang, S.J., 1970. Asymptopic analysis of the modes of wave propagation in a solid cylinder. J. Acoust. Soc. Am. 47, 1282–1289.

Baker, W.E., 1961. Axisymmetric modes of vibration of thin spherical shell. J. Acoust. Soc. Am. 33, 1749–1758.

Baker, W.E. et al., 1966. Elastic response of thin spherical shell to axisymmetric blast loading. J. Appl. Mech., ASME 33, 800–806.

Bieriek, M.P., Freudenthal, A.M., 1962. Forced vibrations of cylindrical sandwich shell. J. Aerospace Sci. 29, 180–184.

Cho, H., Kardomates, G.A., Vally, C.S., 1998. Elastodynamic solution for the thermal shock stresses in an orthotropic thick cylindrical shell. J. Appl. Mech., ASME 65, 184–193.

Chu, H.N., 1961. Vibrations of honeycomb sandwich cylinders. J. Aerospace Sci. 28, 930–939.

Huth, J.H., 1955. Elastic stress waves produced by pressure loads sort on a spherical shell. J. Appl. Mech., ASME 22, 473–478.

Lekniskii, S.G., 1981. Theory of elasticity of an anisotropic body. Moscow Mir Publishers.

Mchinney, J.M., 1971. Spherically symmetric vibration of an elastic spherical shell subjected to a radial and time-dependent body force field. J. Appl. Mech., ASME 38, 702–708.

Miklowitz, J., 1966. Elastic wave propagation. In: Abramson, H.N. et al. (Eds.), Appl. Mech. Surveys. Spartan Books, Washington, p. 809.

Pao, Y.H., 1983. Elastic wave in solid. J. Appl. Mech., ASME 50, 1152–1164.

Piskunov, V.G. et al., 1994. Transverse shear and normal deformation higher-order theory for the solution of dynamic problems of laminated plates and shells. Int. J. Solids Struct. 31 (24), 3345–3374.

Shakeri, M., Eslami, M.R., Yas, M.H., 1999. Elasticity solution and free vibrations analysis of laminated anisotropic cylindrical shells. Struct. Eng. Mech. 7 (2), 181–202.

Torvic, P.J., 1967. Reflection of wave trains in semi-infinite plates. J. Acoust. Soc. Am. 41, 346–353.

Tabiei, A., Tanov, R., Simises, G.J., 1999. Numerical simulation of cylindrical laminated shells under impulsive lateral pressure. AIAA J. 37 (5), 629–633.

Wang, X., Zhang, K., Zhang, W., 2000. Theoretical solution and finite element solution for an orthotropic thick cylindrical shell under impact load. J. Sound Vibr. 236 (1), 129–140.

Yu, Y.Y., 1960. Vibrations of elatic sandwich cylindrical shell. J. Appl. Mech., ASME 82, 653–662.